0.486, deviates even more than ours from the Bloomfield–Zimm value.

Acknowledgment. J.M.G.B. acknowledges a sabbatical research leave awarded by the Ministerio de Educacion y Ciencia. This work was supported by Grants PB87/0694 (J.G.T.), PB86/0012 (J.J.F.), and PB85/0479 (M.M.T.) from the Comision Interministerial de Ciencia y Tecnologia.

References and Notes

(1) Kramers, W. *J. Chem. Phys.* **1946**, *14*, 415.
(2) Zimm. B. H.; Stockmayer, W. H. *J. Chem. Phys.* **1949**, *17*, 301.
(3) Semlyen, J. A., Ed. *Cyclic Polymers*; Elsevier: London, 1986.
(4) Fiers, W.; Sinsheimer, R. L. *J. Mol. Biol.* **1962**, *5*, 408, 424.
(5) Burton, A.; Sinsheimer, R. L. *Science* **1963**, *142*, 962.
(6) Wang, J. C. Reference 3; p 265.
(7) Bloomfield, V. A.; Zimm. B. H. *J. Chem. Phys.* **1966**, *14*, 315.
(8) Zimm. B. H. *J. Chem. Phys.* **1956**, *24*, 269.
(9) Kirkwood, J. G. *J. Polym. Sci.* **1954**, *12*, 1.
(10) Fakatsu, M.; Kurata, M. *J. Chem. Phys.* **1966**, *44*, 4539.
(11) Yamakawa, H. *Modern Theory of Polymer Solutions*; Harper and Row: New York, 1970; Chapter 6.
(12) Zimm, B. H. *Macromolecules* **1980**, *13*, 592.
(13) García de la Torre, J.; Jimenez, A.; Freire, J. J. *Macromolecules* **1982**, *15*, 148.
(14) García de la Torre, J.; Lopez Martínez, M. C.; Tirado, M. C.; Freire, J. J. *Macromolecules*, **1984**, *17*, 2715.
(15) Fixman, M. *J. Chem. Phys.* **1986**, *84*, 4080, 4085.
(16) Roovers, J. *J. Polym. Sci., Polym. Phys. Ed.* **1985**, *23*, 1117.
(17) Kosmas, M. K. *J. Chem. Soc., Faraday Trans. 2* **1988**, *84*, 633.
(18) Candau, F.; Rempp, P.; Benoit, H. *Macromolecules* **1972**, *5*, 627.
(19) Duval, M.; Lutz, P.; Strazielle, C. *Makromol. Chem., Rapid Commun.* **1985**, *6*, 71.
(20) Lutz, P.; McKenna, G. B.; Rempp, P.; Strazielle, C.; *Makromol. Chem., Rapid Commun.* **1986**, *7*, 599.
(21) Hadziionnou, G.; Cotts, P. M.; ten Brinke, G.; Han, C. C.; Lutz, P.; Strazielle, C.; Rempp, P.; Kovacs, A. J. *Macromolecules* **1987**, *20*, 493.
(22) McKenna, G. B.; Hostetter, B. J.; Hadjichristidis, N.; Fetters, L. J.; Plazeck, D. J. *Macromolecules* **1989**, *22*, 1834.
(23) He, Z.; Yuan, M.; Zhang, X.; Wang, X.; Xiaoming, J. *Eur. Polym. J.* **1986**, *22*, 597.
(24) Higgins, J.; Nicholson, L. K.; Hayter, J. B.; Dodgson, K.; Semlyen, J. A. *Polymer* **1983**, *24*, 793.
(25) Edwards, C. J. C.; Richards, R. W.; Stepto, R. F. T.; Dodgson, K.; Higgins, J. S.; Semlyen, J. A. *Polymer* **1984**, *25*, 365.
(26) Clarson, S. J.; Semlyen, J. A.; Stepto, R. F. T. *Polymer* **1986**, *27*, 31.
(27) Chen, Y. *J. Chem. Phys.* **1981**, *71*, 5160.
(28) Baumgartner, A. *J. Chem. Phys.* **1982**, *76*, 4275.
(29) Bruns, W.; Naghizadeh, J. *J. Chem. Phys.* **1976**, *65*, 747.
(30) Freire, J. J.; Pla, J.; Rey, A.; Prats, R. *Macromolecules* **1986**, *19*, 452.
(31) Rey, A.; Freire, J. J.; García de la Torre, J. *Macromolecules* **1987**, *20*, 2385.
(32) García de la Torre, J.; Bloomfield, V. A. *Q. Rev. Biophys.* **1981**, *14*, 81.
(33) García de la Torre, J. In *Dynamic Properties of Biomolecular Assemblies*; Harding, S. E., Rowe, A., Eds.; Royal Society of Chemistry: London, 1989; p 3.
(34) Liu, T. W.; Öttinger, H. C. *J. Chem. Phys.* **1987**, *87*, 3131.
(35) Freire, J. J.; Prats, R.; Pla, J.; García de la Torre, J. *Macromolecules* **1984**, *17*, 1815.
(36) Schaub, B.; Creamer, D. B.; Johannesson, H. *J. Phys. A: Math. Gen.* **1988**, *21*, 1431.

Effect of Swelling on the Fractal Dimension of Branched Silica Polymers Formed near the Sol–Gel Transition[†]

James E. Martin* and Judy Odinek

Sandia National Laboratories, Albuquerque, New Mexico 87185

Received November 10, 1989; Revised Manuscript Received March 10, 1990

ABSTRACT: Scaling theories of semidilute branched polymer solutions depend crucially on the notion that diluted clusters swell sufficiently to alter the fractal dimension. This change in dimension gives rise to the concentration scaling $\xi \sim c^{-5/3}$ of the spatial correlation length ξ. We report light scattering studies of semidilute solutions of silica branched polymers formed near the sol–gel transition that show that the spatial correlation length scales as $\xi \sim c^{-2.0\pm0.3}$, lending credence to the swelling conjecture. The nonequilibrium nature of chemical gels is then demonstrated by comparing the fractal dimension $D \cong 1.6$ of dilution-induced spatial correlations to the fractal dimension $D \cong 1.9$ found when the gel is grown under dilute conditions. In dilute solutions, cluster growth is exponential in time and the system is well described by reaction-limited aggregation.

Introduction

Branched polymers formed near the sol–gel transition have remarkable scaling properties that are only just beginning to be widely appreciated. The variety of static and dynamic scaling behaviors exhibited by branched polymers is striking, particularly in the area of dynamics where qualitatively new effects have been observed. However, to date relatively little work has been done on semidilute solutions. Static scaling investigations of the sol–gel transition have focused primarily on *dilute* solutions, using light[1-3] and neutron[4] scattering to determine both the ensemble and single-polymer fractal dimensions and the critical exponents.[5] These static measurements generally support the percolation description

---

[†] This work was performed at Sandia National Laboratories, Albuquerque, NM, and supported by the U.S. Department of Energy under Contract No. DE-AC-04-76DP00789.

0024-9297/90/2223-3362$02.50/0

of the sol–gel transition, although some discrepancies have been found. On the other hand, dynamic studies, using quasielastic light scattering[6] and viscoelasticity,[7-11] have been done on polymers in the undiluted reaction bath. These dynamical probes reveal an elegant scaling of the dynamics that is related to the absence of a quantifiable time scale at the gel point. Thus some aspects of the scaling of branched polymers in dilute solutions and in the reaction bath are understood.

In this paper, we address the static scaling of branched polymers in semidilute solutions, with regard to the change of cluster fractal dimension upon dilution. Because branched polymers of comparable size do not overlap, this change in dimension is crucial to the scaling of semidilute branched polymers. Contrast this with linear polymer Θ solutions, where the fractal dimension does not change upon dilution, but scaling still occurs due to the overlap of chains.

The appearance of a sizeable spatial correlation length in semidilute solutions leads in a natural way to the consideration of the nonequilibrium nature of chemical gels. To this end we synthesize gels at low initial silica concentration and show that the spatial correlations that evolve are due to reaction-limited cluster–cluster aggregation. Thus diluted branched polymers give a fractal dimension of $D \cong 1.6$, whereas branched polymers grown under dilute conditions give a fractal dimension of $D \cong 1.9$.

Semidilute Solutions

Scale Invariance in Branched Polymers. The semidilute scaling of branched polymers arises from a different physical basis than the more familiar scaling of linear polymers. To appreciate this difference it is helpful to make comparison to linear polymers. Exponents for scaling theories of linear polymers can be expressed in terms of the fractal dimension D of the linear polymer alone (along with the dimension d of space). This fractal dimension varies with the environment, be it a melt ($D = 2$), a good solvent ($D \cong 5/3$), or a Θ solvent ($D = 2$). For example, in terms of the difference $\Delta D = d - D$, the semidilute correlation length of a linear polymer can be expressed as[12] $\xi \sim c^{-1/\Delta D}$, the intrinsic viscosity as[12] $[\eta] \sim M^{\Delta D/D}$, and the osmotic pressure as[12] $\Pi/kT \sim c^{d/\Delta D}$. One can systematically express static scaling quantities in terms of ΔD, since the single-chain fractal dimension is the only fundamental scale invariance exhibited by linear polymers. Thus in the collapsed state, where $D = d$, semidilute scaling is not observed.

In contrast, branched polymers have two fundamental scale-invariant properties: the fractal dimension of a single polymer and the size distribution. These distinct types of self-similarity lead to static scaling expressions that contain not $d - D$, but $\Delta D = D - D_s$, where D is the fractal dimension in the reaction bath and D_s is the swollen fractal dimension in a dilute solution. For example, the semidilute correlation length scales like $\xi \sim c^{-D/d\Delta D}$. Thus scaling in branched polymers is dependent on a change in fractal dimension upon dilution.

The first type of scale invariance exhibited by branched polymers is the fractal nature of a single cluster. In the following, we summarize the simple, mean-field theories of the fractal dimension of branched polymers that have been developed by Isaacson and Lubensky[13] and de Gennes.[14] In the reaction bath, it is thought that two-body interactions between monomers on a cluster are partially *screened* by intervening clusters. These screened clusters have the percolation single-cluster dimension of $D \cong (d + 2)/2$ ($2 \leq d \leq 6$). However, when branched polymers are diluted by a good solvent, two-body interactions within a cluster are unscreened and excluded volume interactions are strong. The fractal dimension D_s of these swollen clusters is then given by the *lattice animal* model, with $D_s = 2(d + 2)/5$ ($d \leq 8$). Lattice animals are the ensemble of all possible branched polymers, each occurring with equal probability, whereas percolation clusters are exponentially weighted by their surface sites—a low probability results from a large surface. (This lattice animal terminology is really incorrect and should not be taken literally. Lattice animals have a *topological dimension* that is distinct from percolation and this dimension is invariant to dilution.[15]) Therefore, in three dimensions it is predicted that the fractal dimension of a *single* branched polymer decreases from 2.5 to 2 upon dilution.

The second form of scale invariance manifested by branched polymers is the size distribution. The incipient gel is a *self-similar distribution* of fractal clusters of all sizes, from monomers to the infinite cluster, as demonstrated by the following derivation of the mass distribution. In order that all clusters see a scale-independent environment, the average separation distance S between clusters of radius $R \pm \mathrm{d} \ln R$ must be proportional to R^1 (this prevents cluster overlap: if $S \sim R^{1+\epsilon}$ small clusters would overlap, and if $S \sim R^{1-\epsilon}$ large clusters would overlap). Using $S \sim 1/N(R)^{1/d} \sim R$ then gives the self-similar distribution $N(R)\,\mathrm{d} \ln R \sim R^{-d} \times \mathrm{d} \ln R$. From the mass fractal formula $R^D \sim m$ the well-known *hyperscaling* relation $N(m)\,\mathrm{d}m \sim m^{-1-d/D}\,\mathrm{d}m$ is then obtained for the mass distribution at the gel point. Slightly away from the gel point the distribution is only self-similar for clusters smaller than the z-average molecular weight M_z: for larger clusters the self-similarity is truncated by an exponential cutoff, giving $N(m)\,\mathrm{d}m \sim m^{-1-d/D}e^{-m/M_z}\,\mathrm{d}m$ or equivalently $N(R)\,\mathrm{d} \ln R \sim R^{-d} \times \exp[-(R/\xi)^D]\,\mathrm{d} \ln R$. Note that linear polymers do not exhibit this second form of self-similarity, since an infinite cluster is not formed in a finite time.

The two forms of scale invariance, cluster dimension and distribution, combine to give an ensemble dimension[16] of $D_e = D(3 - \tau)$. The ensemble dimension, not the single-cluster dimension, determines the scattering properties of a fractal system, with the result $I/c \sim q^{-D_e}$ for $qR \gg 1$ (q is the inverse length $4\pi \sin(\theta/2)/\lambda$, where θ is the scattering angle and λ is the wavelength in the scattering medium). In dilute solution the swollen ensemble dimension is $D_s(3 - \tau) = 2(3 - 2.2) = 1.6$. Intermediate light scattering studies on silica[1,2] have given $I/c \sim q^{-1.6\pm0.06}$, in agreement with this prediction.

Semidilute Crossover. The issue of cluster overlap can be addressed by adding up the individual volumes of all clusters in the reaction bath;[17] $\phi = \int N(R) R^d \times \mathrm{d} \ln R$. For linear polymers the polydispersity is weak (i.e., only a single divergent average mass, $M_w \sim M_z$), so the total chain volume is $\phi \sim M_z^{d/D}$. Since the actual volume occupied by the chains is fixed, the chains must thus completely overlap. The semidilute crossover concentration, c^*, is thus approached by the chains disentangling to fill the available volume of solution: c^* is the point of complete disentanglement. In branched polymers the distribution is $N(R) \sim R^{-d}$ so ϕ increases only logarithmically,[17] $\phi \sim \ln M_z$ (the weak logarithmic divergence only arises because we have neglected the overlap of small clusters with large clusters). Thus the volume fraction of nonoverlapping branched polymers is of order unity in the reaction bath.

In contrast, the semidilute crossover of a branched polymer solution is approached not by disentanglement, but by dilution-induced swelling. This crossover may be defined as the concentration at which swelling is complete[17,18] or, alternatively, as the concentration at which the zero-shear solution viscosity is independent of molecular weight,[9] $c^* \sim 1/[\eta]$ ($[\eta]$ is the intrinsic viscosity). The static calculation of c^* is straightforward: at c^* the total cluster volume is $\phi \sim \int N(m)R^d\,\mathrm{d}m \sim M_z{}^{d(1/D_s-1/D)}$, where the swollen dimension D_s relates the radius to the mass via $R^{D_s} \sim m$. At this solution volume the concentration is $c^* \sim M_z{}^{-d(1/D_s-1/D)}$.

The semidilute crossover can also be obtained[9] by summing the Zimm modes for a single swollen branched polymer and averaging this over the polydisperse ensemble to obtain the shear relaxation modulus $G(t) \sim t^{-D_s/D}f(t/\tau_z)$, where $f(t/\tau_z)$ is small for $t \gg \tau_z$ and $\tau_z \sim M_z{}^{d/D_s}$. Integrating $G(t)$ then gives the intrinsic viscosity $[\eta] \sim M_z{}^{d(1/D_s-1/D)}$ and the inverse of this is c^*.

The concentration scaling of the spatial correlation length[17,18] is obtained by noting that at c^* the correlation length is just the size of a typical swollen cluster, $\xi^* \sim M_z{}^{1/D_s} \sim c^{*-D/d\Delta D}$. The correlation length is then expressed in the scaling form $\xi(c) \sim \xi^* f(c/c^*)$, where in semidilute solutions ξ is expected to be independent of the mean cluster size, $\xi(c) \sim \xi^{*0}$. From this condition and the expression for ξ^* the result

$$\xi \sim c^{-D/d\Delta D} \tag{1}$$

is obtained for $c \gg c^*$.

Scattering in the Semidilute Regime. The semidilute scattered intensity is of the form

$$I/c = aM_w(c)f(q\xi) \tag{2}$$

where $M_w(c)$ is the weight-average molecular weight within a correlation length and a is a constant that combines the effects of various fixed experimental parameters and electromagnetic constants. The weight-average molecular weight is related to the correlation length through the swollen ensemble fractal dimension $M_w \sim \xi^{D_s(3-\tau)} \sim \xi^{8/5}$, giving

$$I/c = a'\xi^{8/5}f(q\xi) \tag{3}$$

The function $f(x)$ has the small-x Guinier expansion $1 - x^2/3$ and in the large-x intermediate scattering regime becomes $x^{-8/5}$, so that for $q\xi \gg 1$, eq 3 reduces to the length-scale-independent form $I/c \sim q^{-8/5}$.

Our light scattering measurements were made very close to the gel point in order to satisfy $q\xi^* \gg 1$. In this regime eq 1 applies, which in three dimensions becomes $\xi = bc^{-5/3}$, where b is a material parameter. Substituting this into eq 3 gives $Ic^{5/3} \sim f(qb/c^{5/3})$, so semidilute scattering data at various concentrations should form a master curve when $Ic^{5/3}$ is plotted versus $qc^{-5/3}$.

Measurement of the Correlation Length. Gels were made from 1 M tetramethoxysilicon combined with 4 M H_2O in methanol. Hydrolysis and condensation were catalyzed with 0.35 mL of 0.109 M NH_4OH in a total sample volume of 25 mL for base gels, and 1.8 mL of 10^{-3} M HCl was used for the acid gels in place of water. After filtration through 0.2-μm filters to remove dust, the samples were placed in a ~50 °C oven to increase the reaction rate. Close to the gel point, the sample was removed from the oven and the reaction was quenched by dilution and cooling to ambient temperature. Light scattering measurements were made with a 50-mW NEC He–Ne laser, from 10 to 135° ($41 < 1/q < 436$ nm), using a 25-mm-diameter Burchard scattering cell in a conventional index-matched scattering vat.

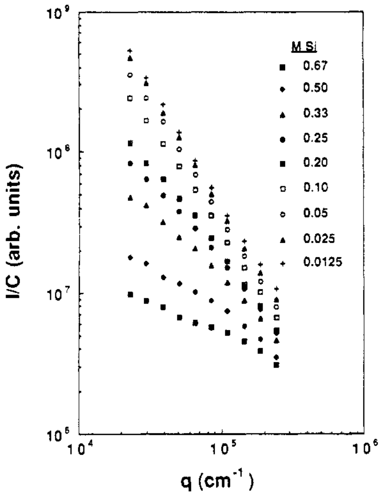

Figure 1. Light scattering data from a 1 M base-catalyzed silica gel diluted very close to the sol–gel transition. At the highest concentration the scattering data are virtually independent of q, indicating that the spatial correlation length is sufficiently small that $q\xi < 1$ in the light scattering regime. At the lowest concentration, intermediate fractal scattering with $I \sim q^{-1.6}$ is observed at all q, demonstrating $q\xi > 1$.

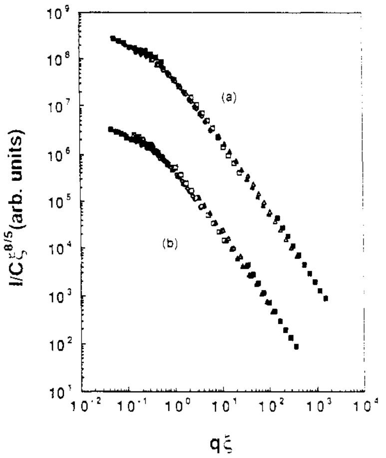

Figure 2. The light scattering data for the base-catalyzed TMOS gel shown in Figure 1 are shown on universal axes appropriately scaled by the correlation length. Curve a was constructed by using the theoretical prediction $\xi \sim c^{-2}$, whereas curve b used the empirical relation $\xi \sim c^{-5/3}$. Both of these scaling assumptions give a good master curve, but larger or smaller exponents did not collapse the data.

Initial experiments gave a poor data collapse because the branched polymers were formed too far from the gel point. In consequence, the criterion $q\xi^* \gg 1$ was not satisfied and power-law scattering of the form $I \sim q^{-1.6}$ was not observed at infinite dilution. Once this pitfall was surmounted, the data shown in Figure 1 were produced for a base-catalyzed gel. In Figure 2b the data are replotted on the universal axes expected from the semidilute scaling ideas presented above, i.e., $Ic^{5/3} \sim f(qc^{-5/3})$. Although this data collapse is acceptable, and so supports the notion that $\xi \sim c^{-5/3}$, other values of y in the expression $\xi \sim c^{-y}$ were investigated in order to attempt to improve the data collapse. Figure 2a shows the marginally improved data collapse obtained with $y = 2$, which gives $Ic^{11/5} \sim f(qc^{-2})$: values of y outside the range of 5/3 to 2 give significantly worse results.

Scattering data for a 1 M acid-catalyzed TMOS gel are shown in Figure 3. With $y = 5/3$ these data give a poor master curve (Figure 4b) but the collapse improves somewhat with $y = 2$ (Figure 4a). The reason for the difference between the scattering behavior of acid- and

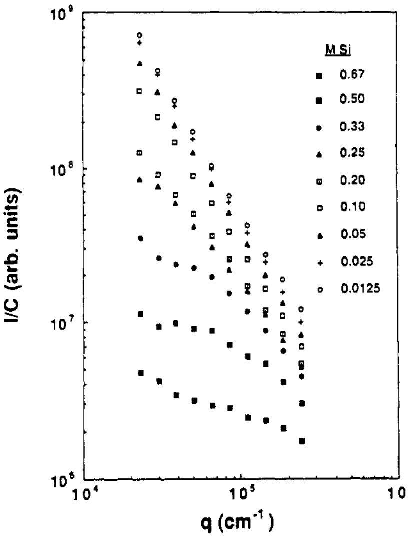

Figure 3. Light scattering data from a 1 M acid-catalyzed silica gel diluted very close to the sol–gel transition. These data are qualitatively similar to those shown in Figure 1 for a base-catalyzed gel, showing a crossover from Guinier to intermediate scattering as the concentration is decreased.

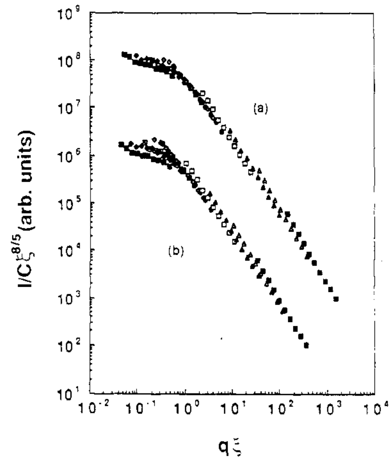

Figure 4. A universal plot of the light scattering data is shown for the acid-catalyzed TMOS gel: curve a was constructed by using $\xi \sim c^{-2}$ and curve b used $\xi \sim c^{-5/3}$. Although the exponent 5/3 does not give a collapse, 2 gives a reasonable master curve.

base-catalyzed gels is not understood, but the growth studies indicate that structural differences arise at early times. These could lead to nonasymptotic crossover effects.

Nonequilibrium Effects: Aggregation versus Percolation

Irreversible Growth. The irreversibility of chemical gels leads to some interesting nonequilibrium structural effects and to questions about the applicability of equilibrium and kinetic growth models to these systems.[19] In short, the nonequilibrium growth of dilute gels in dilute solution gives rise to a correlation length and semidilute crossover that are not to be confused with the ξ and c^* that arise from dilution of clusters. In the following, we demonstrate that the early-time growth of clusters in a dilute gelling medium is described by aggregation and that only when the semidilute condition for aggregation is reached does the system cross over to percolation.

Because of irreversibility, the structure of chemical gels is not a function of state variables such as the temperature, composition, etc. but depends on the preparative path. For example, it is possible to produce an *incipient* 0.25 M TMOS gel by approaching the gel point along each of the two paths shown in Figure 5: either one can react a 1.0 M TMOS to the gel point and then dilute by a factor of 4 or one can directly react 0.25 M TMOS to the gel point. Scattering data for each of these cases are compared in Figure 6, where a greater fractal dimension is observed for the gel that was allowed to grow under more dilute conditions. In early SAXS measurements on silica,[23] the dependence of the fractal dimension on preparative path was not appreciated, and the fractal dimension of ~2 that was observed on length scales smaller than 5.0 nm was attributed to lattice animals rather than aggregation.

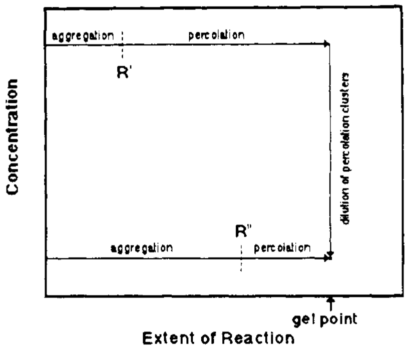

Figure 5. Two possible preparative pathways in chemical gel formation are shown schematically. Reaction under dilute conditions gives an extensive aggregation regime, marked by exponential growth of clusters with $D_a \cong 2$ that persists until clusters attain a radius of $R'' \sim 1/\phi_0^{1/(d-D_a)}$. At this critical size, the system becomes semidilute and crosses over to percolation with its associated critical growth. Since percolation is a connectivity transition, spatial correlations formed along this path are solely due to aggregation. Under more concentrated conditions, the aggregation regime is truncated ($R' \ll R''$) and growth is dominated by percolation. When these percolation clusters are diluted, spatial correlations of dimension 1.6 develop due to the swelling of percolation clusters.

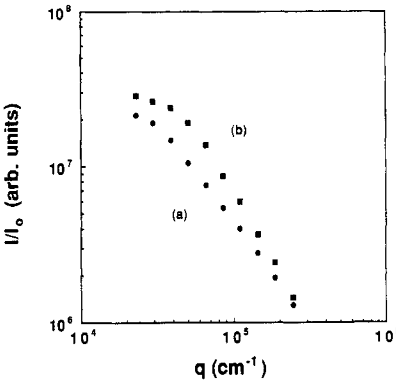

Figure 6. Light scattering data for samples brought to the gel point along the two paths illustrated in Figure 5 indicate a significant difference in structure, although the data are too cose to $qR \cong 1$ to be definitive. Curve a is for an acid-catalyzed gel grown to the gel point at a concentration of 1 M TMOS and then diluted to 0.25 M, whereas curve b is a for a gel brought to the sol–gel transition at 0.25 M TMOS. As expected, curve b is more dominated by aggregation and the scattering data thus have a steeper slope at large q, indicating a higher fractal dimension. This point is further pursued in Figure 8.

Exponential Growth of Clusters. The difference between structures produced by different preparative routes can be understood by considering the kinetic aspects of growth in silica. When polycondensation of dilute TMOS is initiated with an acid or base catalyst, the methoxy groups are hydrolyzed, producing reactive hydroxyl groups which then condense to form Si–O–Si bonds. Under conditions where the rate of hydrolysis is very high, the

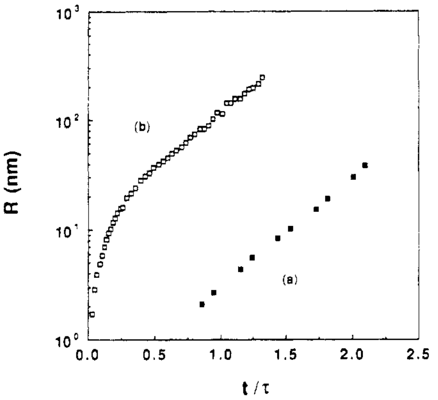

Figure 7. Experimental evidence for reaction-limited aggregation (RCLA) comes from early-time studies of cluster growth. Curve a is an acid-catalyzed 0.1 M TMOS gel that shows exponential growth from the earliest times. Curve b is a base-catalyzed gel that shows the formation of colloids of radius ~20 nm before the exponential growth characteristic of RCLA is observed.

limited solubility of silicic acid makes it possible to produce supersaturated solutions where growth is initiated by nucleation, producing small silica colloids that may then aggregate to form a gel. Under less aggressive hydrolysis conditions, however, monomers condense to form ramified clusters. In this case, X-ray scattering measurements do not show the q^{-4} Porod's law scattering characteristic of hard surfaces, so there is no evidence for colloid formation. Depending on the activation energy of the forward reaction, the clustering of monomers or colloids may be either reaction- or diffusion-limited: in the TMOS systems considered here, the growth is always in the slow, reaction-limited regime. Furthermore, since the reaction is essentially irreversible, the randomness is quenched on the experimental time scale.

Experimental evidence for aggregate formation is shown in Figure 7, where early-time growth data for acid- and base-catalyzed gels are compared. The acid-catalyzed data show exponential growth from the earliest times, in accord with experimental findings[20-22] for slow aggregation of silica. The base-catalyzed data show evidence of colloid formation[19] at very short times but then cross over to exponential growth as the colloidal particles aggregate under reaction-limited conditions. In the base-catalyzed system the exponential growth starts at a radius of 20 nm, which is probably a good estimate of the colloid size, whereas in the acid-catalyzed gel a radius of <2 nm is indicated.

Intermediate Scattering. Extensive studies of slow aggregation of aqueous silica colloids under dilute conditions show that fractal aggregates of dimension $D_a = 2.05 \pm 0.06$ are formed.[20-22] The fraction of the solution volume occupied by these clusters increases with the cluster radius R as $\phi = (R/b)^{d-D_a}\phi_0$, where ϕ_0 is the initial monomer volume fraction and b is the monomer radius. The semidilute condition is attained when $\phi = 1$, at which point the cluster radius is $R^\dagger = b/\phi_0^{1/(d-D_a)}$. The spatial correlation length then remains pinned at $R^\dagger$ unless the system is diluted;[19] further growth is due to percolation of these semidilute aggregates, but this does not affect the undiluted structure. Thus scattering measurements on a gel prepared under initially dilute conditions should exhibit spatial correlations due to aggregation, with intermediate scattering of the form $I \sim q^{-2.05\pm0.06}$. The relatively steep slope of the scattering data in Figure 6b indicates that reaction-limited aggregation may indeed account for the structure of the gel grown under dilute conditions. Since these data do not satisfy the intermediate scattering criterion $qR \gg 1$, the crossover to Guinier scattering at small q obscures the scaling behavior.

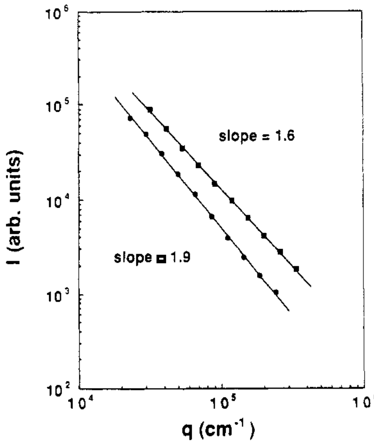

Figure 8. In order to exaggerate the structural differences between dilute and diluted gels, a base-catalyzed gel was grown at 0.1 M TMOS. Growth was allowed until 500-nm clusters were formed and without dilution, intermediate scattering data in curve a showing a slope of 1.9 were obtained, indicating RCLA. Another base-catalyzed sample was prepared at 1.0 M TMOS, brought to the gel point, and diluted 250:1 to obtain the intermediate scattering data in curve b. The observed dimension of 1.6 indicates swollen percolation clusters.

In order to obtain more accurate structural information in the dilute, nonequilibrium growth regime, a base-catalyzed 0.1 M TMOS gel was prepared in methanol. When the clusters were sufficiently large that $qR \gg 1$, the intermediate light scattering measurements in Figure 8 were made, which show mass fractal behavior with a dimension of $D \cong 1.9$, in good agreement with studies of the aqueous[20-22] aggregation of commercial colloidal silica.

On the other hand, when a gel is produced under concentrated conditions, growth crosses over from aggregation to percolation at a much smaller value of $R^\dagger$. If $qR^\dagger \ll 1$ in the light scattering window (the undiluted data in Figure 1 demonstrate $qR^\dagger \ll 1$ for 1 M TMOS), then the spatial correlations produced by diluting the sample should be described by the swollen ensemble dimension for percolation, with $I \sim q^{-1.6\pm0.06}$, and the data in Figure 6a do indicate a smaller dimension than that of aggregation. This point is pursued in Figure 8, where data taken purely in the intermediate scattering regime give $I \sim q^{-1.60\pm0.06}$ for a 1 M base-catalyzed silica gel diluted 250:1 near the gel point. These data indicate that chemical gelation in dilute solutions manifests aspects of both kinetic and equilibrium growth. Dilution studies allow investigation of the equilibrium structures formed in the connectivity divergence, whereas studies of initially dilute systems reveal structures formed by aggregation.

Conclusions

From static light scattering measurements we have shown that branched silica polymers formed near the sol-gel transition show scaling in the semidilute regime. The spatial correlation length was found to obey $\xi \sim c^{-2.0\pm0.3}$, in reasonable agreement with the theoretical prediction $\xi \sim c^{-5/3}$, with a slightly larger exponent for the acid-catalyzed system. These spatial correlations are dilution-induced and apparently arise from the swelling of the equilibrium ensemble of percolation clusters. Intermediate light scattering experiments show that this ensemble has a fractal dimension of 1.6 ± 0.06.

The nonequilibrium nature of chemical gels was subsequently demonstrated by allowing cluster formation to occur under dilute growth conditions. Quasielastic light scattering measurements then reveal exponential growth in time, as opposed to the critical growth observed close to the gel point. This exponential growth and the observed dimension of $D \cong 2$ indicate nonequilibrium cluster formation via reaction-limited aggregation. Thus different preparative pathways can be used to modify the structure of silica gels.

References and Notes

(1) Martin, J. E. In *Time-Dependent Effects in Disordered Materials*; Pynn, R., Riste, T., Eds.; Plenum: New York, 1988.
(2) Martin, J. E.; Keefer, K. D. *Phys. Rev. A* **1986**, *34*, 4988.
(3) Dubois, M.; Cabane, B. *Macromolecules* **1989**, *22*, 2526.
(4) Bouchaud, E.; Delsanti, M.; Adam, M.; Daoud, M.; Durand, D. *J. Phys. (Paris)* **1986**, *47*, 1273.
(5) Martin, J. E.; Wilcoxon, J. P.; Adolf, D. *Phys. Rev. A* **1987**, *36*, 1803.
(6) Martin, J. E.; Wilcoxon, J. P. *Phys. Rev. Lett.* **1988**, *61*, 373.
(7) Chambon, F.; Winter, H. H. *Polym. Bull.* **1985**, *13*, 499. See also: Chambon, F.; Winter, H. H. *J. Rheol.* **1987**, *31*, 683.
(8) Martin, J. E.; Adolf, D.; Wilcoxon, J. P. *Phys. Rev. Lett.* **1988**, *61*, 2620.
(9) Martin, J. E.; Adolf, D.; Wilcoxon, J. P. *Phys. Rev. A* **1989**, *39*, 1325.
(10) Durand, D.; Delsanti, M.; Adam, M.; Luck, J. M. *Europhys. Lett.* **1987**, *3*, 297.
(11) Adolf, D.; Martin, J. E.; Wilcoxon, J. P. *Macromolecules* **1990**, *23*, 527.
(12) de Gennes, P.-G. *Scaling Concepts in Polymer Physics*; Cornell University Press: Ithaca, NY, 1979.
(13) Isaacson, J.; Lubensky, T. C. *J. Phys. (Paris)* **1980**, *41*, L469.
(14) de Gennes, P.-G. *J. Phys. (Paris)* **1979**, *40*, L197.
(15) Martin, J. E. *J. Phys. A: Math. Gen.* **1985**, *18*, L207.
(16) Martin, J. E.; Ackerson, B. J. *Phys. Rev. A* **1985**, *31*, 1180. See also: Martin, J. E. *J. Appl. Crystallogr.* **1986**, *19*, 25.
(17) Daoud, M.; Martin, J. E. In *The Fractal Approach to Heterogeneous Chemistry: Surfaces, Colloids, Polymers*; Avnir, D., Ed.; Wiley: London, 1989.
(18) Daoud, M.; Leibler, L. *Macromolecules* **1988**, *21*, 1497.
(19) Martin, J. E.; Wilcoxon, J. P. *Phys. Rev. A* **1989**, *39*, 252.
(20) Martin, J. E. *Phys. Rev. A* **1987**, *36*, 3415.
(21) Aubert, C.; Cannell, D. S. *Phys. Rev. Lett.* **1986**, *56*, 738.
(22) Schaefer, D.; Martin, J. E.; Cannell, D.; Wiltzius, P. *Phys. Rev. Lett.* **1984**, *52*, 2371.
(23) Schaefer, D.; Keefer, K. D. *Phys. Rev. Lett.* **1984**, *53*, 1383.

Exchange Kinetics between the Adsorbed State and Free Solution: Poly(methyl methacrylate) in Carbon Tetrachloride

Harry E. Johnson and Steve Granick*

Department of Materials Science and Engineering, University of Illinois, Urbana, Illinois 61801

Received November 3, 1989

ABSTRACT: Adsorption and desorption rates at high surface coverage are reported for poly(methyl methacrylate) (PMMA) adsorbed from dilute carbon tetrachloride solution (1 mg·mL^{-1}) onto a single silicon oxide substrate at 30.0 °C. The method of measurement was infrared spectroscopy in attenuated total reflection. The polymer fractions studied were deuterio (d-PMMA) and protio (h-PMMA) with matched degrees of polymerization $N_w \approx 570$ and 640, respectively. No adsorption isotope effect was expected, nor noted experimentally. The rapid adsorption of d-PMMA onto the initially bare surface was followed for 1 h, at which time the ambient solution was changed either to a solution of h-PMMA or to pure CCl_4. Desorption of d-PMMA after this time was linear in the elapsed time over 6 h, with rate on the order of 1% h^{-1}, and this rate was the same into a solution of h-PMMA as into pure CCl_4 at 30 and 40 °C. The infrared bound fraction, i.e., the fraction of segments in direct contact with the surface, was also measured. During adsorption onto initially bare surfaces, the average bound fraction took the constant level $p \approx 0.25$ throughout the experiments. However, for h-PMMA penetrating the preadsorbed d-PMMA layer after this polymer was allowed to adsorb for 1 h, the average bound fraction was $p \approx 0.1$ at elapsed times of minutes but rose to $p \approx 0.2$ after 6 h. This indicates that incoming chains underwent spreading at the surface. Control experiments with stearic acid in CCl_4 showed that adsorption–desorption kinetics in this system were more rapid than the experimental time scale. This suggests that despite slow rearrangements of the overall chains, rearrangements may have been rapid at the level of individual segments. The surface excess adsorbed amount in this PMMA system was dominated by sluggish relaxation and, by inference, by metastable nonequilibrium states.

Introduction

What physical picture should one imagine of polymers at a surface? It has long been known that the mass adsorbed usually amounts to more than a monolayer of repeat units; therefore presumably the segments of chains between adsorption sites loop into solution. Much theoretical attention has been given to describing the spatial distribution of segments at equilibrium. Tails at the ends of the macromolecules dangle dozens or hundreds of angstroms into solution; loops of various sizes also dangle into solution; and the entire structure is anchored to the surface by only a fraction of the potential adsorption sites. The resulting concentration profile decays roughly exponentially with distance from the surface, and its characteristic thickness is predicted to be of the same order as the correlation length. For polymers adsorbed from dilute solution, this distance is of the same order as the radius of gyration of an isolated chain in solution. On the experimental side, information of a definitive quan-

0024-9297/90/2223-3367$02.50/0